frontiers | Frontiers in Earth Science

TYPE Original Research
PUBLISHED 13 January 2023
DOI 10.3389/feart.2022.1033541

OPEN ACCESS

EDITED BY
Fan Yang,
Lanzhou University, China

REVIEWED BY
Wang Guangzeng,
Ocean University of China, China
Min Liu,
Northwest University, China
Liang Qiu,
China University of Geosciences, China

*CORRESPONDENCE
Chang-Hao Xiao,
xiaochanghao1986@126.com

SPECIALTY SECTION
This article was submitted to Structural Geology and Tectonics, a section of the journal Frontiers in Earth Science

RECEIVED 31 August 2022
ACCEPTED 01 November 2022
PUBLISHED 13 January 2023

CITATION
Hu J-X, Xiao C-H, Wei C-S, Shen Y-K, Chen Z-L, Zhang Y and Zhang D (2023), Polyphase deformation of the Youjiang fold-and-thrust belt during the Mesozoic: Implications for the tectonic transition of the South China block. *Front. Earth Sci.* 10:1033541. doi: 10.3389/feart.2022.1033541

Polyphase deformation of the Youjiang fold-and-thrust belt during the Mesozoic: Implications for the tectonic transition of the South China block

Jia-Xiu Hu[1,2], Chang-Hao Xiao [2,3]*, Chang-Shan Wei[2,3], Yu-Ke Shen[2,3], Zheng-Le Chen[2,3], Yu Zhang[1,2] and Da Zhang[1]

[1]School of Earth Sciences and Resources, China University of Geosciences (Beijing), Beijing, China, [2]Laboratory of Dynamic Diagenesis and Metallogenesis, Institute of Geomechanics, Chinese Academy of Geological Sciences, Beijing, China, [3]Key Laboratory of Paleomagnetism and Tectonic Reconstruction, Ministry of Natural Resources, Beijing, China

The South China block (SCB) experienced the tectonic transition from the Paleo-Tethys to the Paleo-Pacific tectonic domains during the Mesozoic, but the transition process is hotly debated. The Youjiang fold-and-thrust belt (YFTB), in the interior of the Youjiang Basin in the southwestern SCB, is located in a junction of these two tectonic domains and thus witnessed their tectonic evolution. It also separates the northern thin-skinned structures from the southern thick-skinned structures in the basin. Therefore, the YFTB is an intriguing window into the Mesozoic evolution in the southwestern SCB and the Mesozoic tectonic transition of the SCB. In this study, we conduct structural analysis at the middle of the YFTB and discuss the Mesozoic tectonic transition of the SCB. Four phases of deformation are identified in the YFTB during the Mesozoic. The first phase of deformation (D_1) is characterized by a series of conjugate joints, NW–SE trending thrust faults and folds resulting from NE–SW shortening that was related to the collision between the SCB and Indochina block. The second phase of deformation (D_2) is manifested by the pre-existing NW–SE striking thrust faults transformed to normal faults and the Late Triassic mafic magmatism. Our structural observations, combined with previous geochronological data for mafic dykes, suggest the study area experienced post-orogenic extension in the Late Triassic. The third phase of deformation (D_3), accompanied with the westward subduction of the Paleo-Pacific oceanic plate, is represented by a series of conjugate joints and NE–SW-striking faults formed by NW–SE compression. As a result of the continuous subduction of the Paleo-Pacific plate and its subsequent slab rollback, the fourth phase of deformation (D_4) is featured with normal faults, magmatic-hydrothermal activities, and regional mineralization, which are associated with the nearly E–W extension setting. Our study results indicate that, in the Early Mesozoic, the Youjiang Basin was dominated by the Paleo-Tethys domain and then transitioned to the Paleo-Pacific domain. Together with the magmatic lull between the Triassic and the

Early-Middle Jurassic identified in the SCB, we propose that the tectonic transition process manifested in the YFTB more likely initiated in the Early Jurassic.

KEYWORDS

Paleo-Tethys, Paleo-Pacific, structural analysis, South China block, Youjiang fold-and-thrust belt

Introduction

The South China block (SCB), as an important component of southeastern Asia, is located at a junction impacted by the Paleo-Tethys and Paleo-Pacific tectonic domains (Figure 1A). During the Late Paleozoic-Mesozoic, the SCB experienced both the assembly of the Indochina block and the SCB and the subduction of Paleo-Pacific plate, triggering tectonic transition and extensive tectono-magmatic activities (Zhang et al., 2013, Zhang D.et al., 2021; Xiao et al., 2018, 2022). The Mesozoic tectonic superposition and transition of the SCB have attracted much attention and prompted numerous studies (Li and Li, 2007; Zhang et al., 2012; Li et al., 2014; Shu et al., 2021). However, the tectonic transition process, especially its initiation timing, is still in dispute (Zhou et al., 2006; Li and Li, 2007; Chen et al., 2008; Wang et al., 2013; Xu et al., 2019). One opinion is that, based on the statistics of the granite ages and types in the SCB, the subduction began in the Late Permian through flat-slab subduction (Li and Li, 2007). This perspective seems to be feasible in relation to some further studies both on magmatism and deformation (Li et al., 2012; Meng et al., 2012). Others have argued that the transition occurred in the Mesozoic, varying from the Late Triassic (Jiang et al., 2015; Xu et al., 2019), the Early Jurassic (Sun et al., 2005; Zhou et al., 2006; Xu et al., 2017), the Middle–Late Jurassic (Wang et al., 2013), to the Cretaceous (Chen et al., 2008). One of the reasons for this controversy is the superposition and complexity of the structural deformation of the two tectonic domains. Hence, distinguishing the deformation sequence is important to elucidate the transition process and onset timing of the SCB.

The Youjiang Basin, as a part of the southwestern margin of the SCB, is situated at the intersection of the Cathaysia, Yangtze, and Indochina blocks (Figure 1B). It is a superimposed location affected by Paleo-Tethys and Paleo-Pacific domains and strongly reworked during the Permian to the Triassic (Chen and Zeng, 1990; Zeng et al., 1995). Due to its particular position, knowledge regarding the evolution of the Youjiang Basin is critical to better understand the Mesozoic tectonic regime transition of the SCB. However, the ambiguity of the geodynamic setting of the Youjiang Basin hinders our understanding of its tectonic evolution. The Triassic Youjiang Basin has generally been recognized as a foreland basin connected with the closure of the Paleo-Tethys Ocean and the succeeding collision between the SCB and the Indochina block (Du et al., 2013; Hu et al., 2015; Lehrmann et al., 2015; Qiu et al., 2016), whereas other studies have suggested that it was a back-arc basin in response to the subduction of the Paleo-Tethys (Chen and Zeng, 1990; Zeng et al., 1995) or the Paleo-Pacific plate (Duan et al., 2020; Wang et al., 2020, 2021).

The structural characteristics of the Youjiang Basin are featured by a progressive deformation from thick-skinned hinterland belt to thin-skinned foreland belt due to the Indosinian orogeny, and these two types of deformation were divided by the Nanpanjiang–Youjiang fault. The earlier structures resulting from the Indosinian tectonic event were transformed in the Yanshanian tectonic event, represented by the N- to NE-striking cleavage and the curving of the Indosinian fold axes (Yang et al., 2021). However, Li et al. (2017) identified that the NE-striking structures related to the subduction of the Paleo-Pacific plate overprinted the NW-striking structures in the Long'an area, the junction of the Youjiang and Shiwandashan structural belts, indicating that the subduction of Paleo-Pacific plate preceded and facilitated the closure of the Paleo-Tethys Ocean. The lack of detailed deformation analysis of these two tectonic domains makes the Mesozoic tectonic setting of the Youjiang Basin poorly constrained and limits our understanding of the tectonic transition of the SCB. Therefore, reconstructing the deformation sequence of the YFTB is conducive to comprehensively discerning the Mesozoic tectonic evolution of the basin and constraining the tectonic transition process of the SCB.

In this contribution, we conduct structural analysis on the geometry and kinematics characteristics of different stages of structures, including faults, folds, and conjugate joints in the YFTB. Combined with regional geology and detailed structural mapping, the results are used to recognize the Mesozoic tectonic evolution of the YFTB and, moreover, elucidate the Mesozoic tectonic transition process of the SCB.

Regional geology

Geological setting

The SCB is formed by the amalgamation of the Yangtze and Cathaysia blocks along the Jiangnan Orogenic belt during the early Neoproterozoic (Lin et al., 2008; Wang et al., 2010, 2013; Zhang et al., 2013; Shu et al., 2021). It is adjacent to the Pacific Ocean and linked to the North China block by the Qinling–Dabie Orogenic belt in the north, the Indochina block by the Song Ma

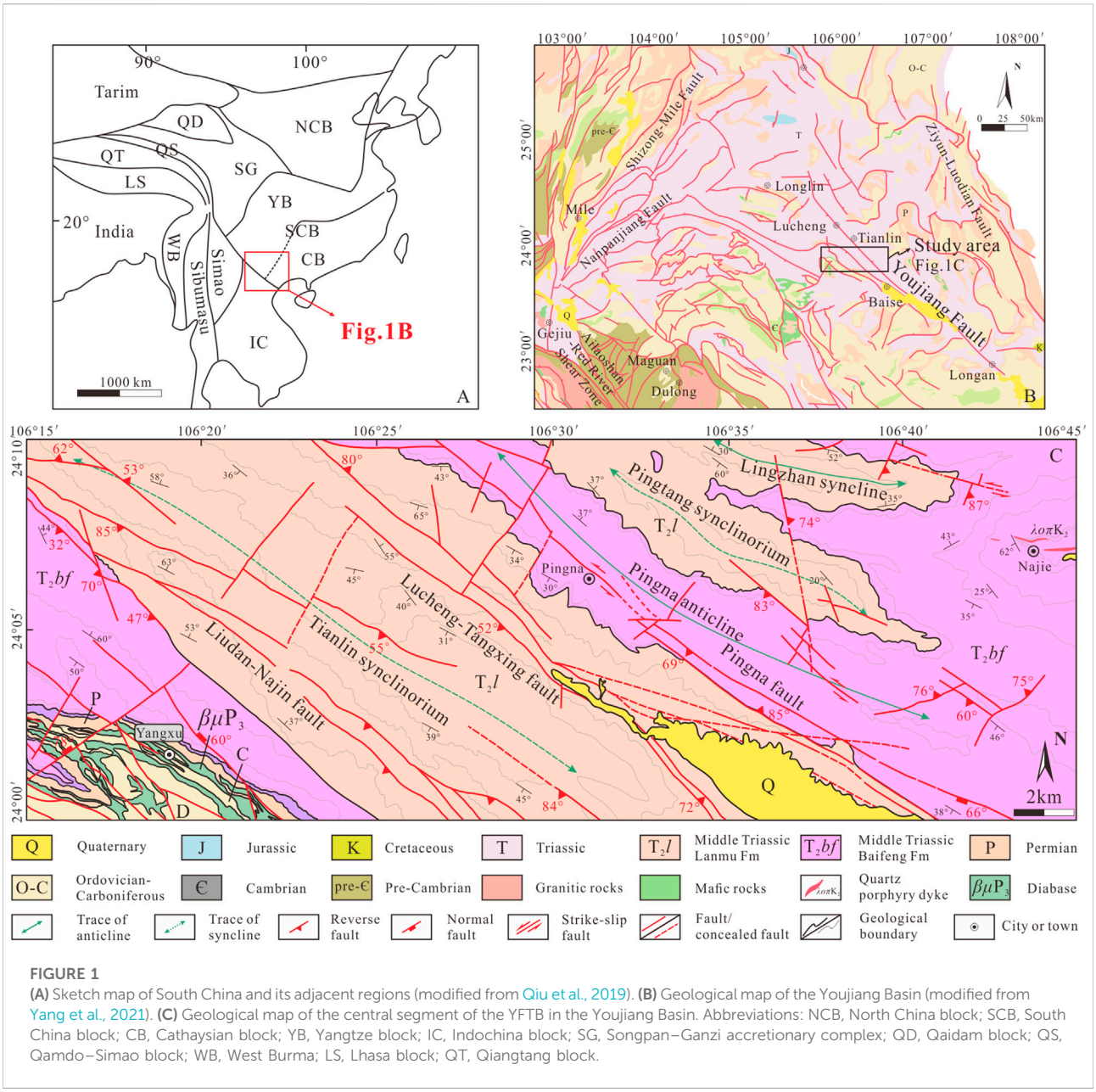

FIGURE 1
(A) Sketch map of South China and its adjacent regions (modified from Qiu et al., 2019). **(B)** Geological map of the Youjiang Basin (modified from Yang et al., 2021). **(C)** Geological map of the central segment of the YFTB in the Youjiang Basin. Abbreviations: NCB, North China block; SCB, South China block; CB, Cathaysian block; YB, Yangtze block; IC, Indochina block; SG, Songpan–Ganzi accretionary complex; QD, Qaidam block; QS, Qamdo–Simao block; WB, West Burma; LS, Lhasa block; QT, Qiangtang block.

suture in the southwest, and the Longmenshan fault zone by the Tibetan Plateau in the west, respectively (Figure 1A). During the Phanerozoic, the SCB was dominated by three tectonic events that are known as the Early Paleozoic intracontinental orogeny between the Yangtze and Cathaysia blocks (the Caledonian tectonic event), the Permian–Triassic continental collision between the SCB and the Indochina block during the Early Triassic (the Indosinian tectonic event) and the Jurassic–Cretaceous Paleo-Pacific plate subduction beneath the SCB (the Yanshanian tectonic event) (Wang et al., 2013; Faure et al., 2014; Xiao et al., 2022; Qiu et al., 2020; Yang et al., 2021).

The Youjiang Basin in the southwestern margin of the SCB is a superimposed location affected by the Tethys tectonic domain, Paleo-Pacific tectonic domain, and Tibetan tectonic domain (Wang et al., 2021). It is a foreland basin bounded by the ShiZong–MiLe fault belt in the northwest, the Ziyun–Luodian fault belt in the northeast, the Ailaoshan–Red River shear zone in the southwest, and the Pingxiang–Nanning fault belt, with the Shiwandashan Basin in the southeast (Figure 1B; Xiao et al., 2018). The basin consists of a pre-Cambrian to Ordovician basement covered by Devonian to Triassic strata (Yang et al., 2020). The major faults are well-developed in NW–NWW-

striking and NE-striking (Chen and Zeng, 1990). They were mostly formed as syn-sedimentary normal faults along the initial rifting of the basin in the Early Devonian (Zeng et al., 1995; Du et al., 2013), and then underwent various movements corresponding to different tectonic events (Wang et al., 2013).

From the Early Devonian to the Early Triassic, the Youjiang Basin was initiated as a rifted basin and gradually developed into a back-arc basin corresponding to the opening of the Ailaoshan Ocean and its subsequent subduction (Zeng et al., 1995). Consequently, the Early Devonian to Early Triassic sedimentation of Youjiang Basin is characterized by the coexistence of deep-water facies, mainly comprising pelite, chert, limestone, and shallow-water facies that primarily include limestone, bioclastic limestone, marlstone, and conglomerates (Du et al., 2013). During the Middle Triassic, accompanied by the closure of the Paleo-Tethys Ocean and the convergence of the Indochina block and SCB along the Song Ma Suture, the Youjiang Basin evolved into a foreland basin, with massive thick Triassic terrigenous turbiditic units consisting of marlstone, mudstone, siltstone, and sandstone (Yang et al., 2020).

Felsic rocks in the Youjiang Basin are mainly exposed along the basin boundary. Minor quartz porphyry dykes and most (ultra-) mafic rocks are revealed in the interior of the basin (Jiang et al., 2019; Qiu et al., 2019; Yang et al., 2020). Previous studies have reported Permian–Early Jurassic mafic rocks with ages of ca. 269–183 Ma and Late Cretaceous mafic and quartz porphyry dykes in northwestern Guangxi and southwestern Guizhou with ages of ca. 100–80 Ma (Chen et al., 2012; Zhu et al., 2017; Xiao et al., 2018; Qiu et al., 2019).

Geology of the Youjiang fold-and-thrust belt (YFTB)

The YFTB is a major fault zone in the interior of the Youjiang Basin, and it begins at Longlin, extending over 360 km through Tianlin and Baise to Nanning. In the northern segment, the YFTB occurs as one main fault, whereas the southern segment is divided into three to five secondary parallel faults from Baise to Nanning, with the whole belt striking NW and steeply dipping to the northeast (Wang et al., 2013). A previous study on the geophysics and structural geology showed that the YFTB, with an overall framework of NE-verging thrusting, produced duplex and imbricate structures in deep and shallow levels respectively. It cut through pre-Cambrian metamorphic basement and Cambrian to Triassic strata and formed a thick-skinned structure. In contrast, the basement on the northeast of the YFTB was not involved in the deformation, indicating a thin-skinned structure (Yang et al., 2021).

The sedimentary rock in the middle of the YFTB is primarily comprised of Devonian, Carboniferous, and Permian and Triassic rocks. The Paleozoic rocks are locally outcropped in the southwest of the study area and primarily comprise carbonate, chert, and mudstone (Figure 1C). The Middle Triassic clastic rocks are the main exposed rocks in the middle of the YFTB and comprise the Middle Triassic Baifeng Formation (T_2bf) and Lanmu Formation (T_2l). The Middle Triassic Baifeng Formation (T_2bf) in the study area includes sandstone, siltstone intercalated with mudstone, and argillaceous siltstone, and the Lanmu Formation (T_2l) is composed of calcareous mudstone, siltstone, and sandstone (Figure 1C). The middle of the YFTB consists of a series of sub-parallel secondary faults, including the Liudan–Najin, Lucheng–Tangxing, and Pingna faults. They strike northwest and dip steeply toward the northeast at high angles of 60°–85° (Figure 1C). A series of folds developed along the fault zone, such as the Tianlin synclinorium, the Pingna anticline, the Pingtang synclinorium, and the Lingzhan syncline. The Tianlin synclinorium is a NW-trending tight fold with a sub-vertical axial plane and a slightly curved hinge, with a core of the Lanmu Formation (T_2l) and limbs of the Baifeng Formation (T_2bf). The Pingna anticline is a secondary fold in the Tianlin synclinorium, cored by the Baifeng Formation (T_2bf) with limbs of the Lanmu Formation (T_2l). It is a NW-trending inclined open fold with southwestern limbs dipping at 25°–50° and northeastern limbs dipping at 60°–80°, and tension joints are well developed in its core. The Pingtang synclinorium is a NWW-trending fold with a curved hinge, a core of the Lanmu Formation (T_2l), and limbs of the Baifeng Formation (T_2bf). The Lingzhan syncline is a NWW-trending fold with steeply-dipping northeastern limbs and moderately-dipping southwestern limbs. It is cored by the Lanmu Formation (T_2l) with limbs of the Baifeng Formation (T_2bf) (Figure 1C). Sporadic magmatic rocks are exposed in the study area, including Early Triassic and Early Jurassic post-orogenic mafic rocks in Badu and Yangxu areas along the Youjiang fault, and Late Cretaceous quartz porphyry dykes in Najie area that formed in the extensional setting (Chen et al., 2012; Zhu et al., 2017; Qiu et al., 2019). A previous study has suggested concealed intrusions in depth based on the regional gravity and magnetic anomalies (Chen et al., 2012).

Methods

The tectonic transition process and evolution can be well archived in the paleo-tectonic stress field in existing structural features and the paleo stress field inversion based on the statistics and analysis of slip vectors is an effective way to determine the paleo-tectonic stress field (Angelier, 1984). The dipping direction and angle of fault planes and the strike and pitch of the striations on fault planes were measured. The sense of movement was determined by mineral steps and syntectonic minerals. The fault-slip vector data were analyzed using FaultKin™ software and listed in Supplementary Table S1 (Allmendinger, 2002).

The conjugate joints were also measured for structural analysis. The orientation of the acute angle bisector between the joints indicates the maximum principal compression stress

FIGURE 2
Field photographs of main structures developed in the D_1 deformation in the YFTB. **(A)** The fold in the siltstone of the Triassic Baifeng Formation at PN2009 indicating a top-to-the-NE movement. **(B)** Asymmetric fold in the siltstone of the Triassic Lanmu Formation at PN2044 indicating a top-to-the-SW movement. **(C)** Asymmetric fold involving the Triassic Lanmu Formation in the Tianlin synclinorium at PN2059 indicating a top-to-the-NE movement. **(D)** Asymmetric fold in the siltstone of the Triassic Baifeng Formation at PN2036 showing a top-to-the-NE movement. **(E)** NE-verging thrusts and fault-related folds involving siltstone of the Triassic Baifeng Formation in the Tianlin synclinorium at PN2007 indicating a top-to-the-NE movement. **(F)** Asymmetric folds involving the siltstone of the Triassic Lanmu Formation in the Tianlin synclinorium at PN2043 demonstrating a NE–SW oriented shortening. **(G)** Asymmetric fold in Triassic siltstone in bedding siltstone of the Triassic Baifeng Formation at PN2032 indicating a top-to-the-NE movement. **(H)** Strike-slip striations on the NWW-striking fault plane indicating a NE–SW compression. **(I)** Sinistral striations and mineral steps in the siltstone of the Triassic Baifeng Formation at PN2057 showing a sinistral strike-slip movement. **(J)** Thrusting striations on the siltstone of the Triassic Baifeng Formation in the Pingna underground tunnel at YM1-11 indicating a NE–SW compression. **(K)** Thrusting striations and mineral steps on the siltstone of the Triassic Baifeng Formation at PN2103 indicating a NE–SW compression. **(L)** Steeply-dipping cleavage (S_1) and structural transposition in the Triassic weakly competent argillaceous siltstones at PN2030 indicating an interlayer shearing.

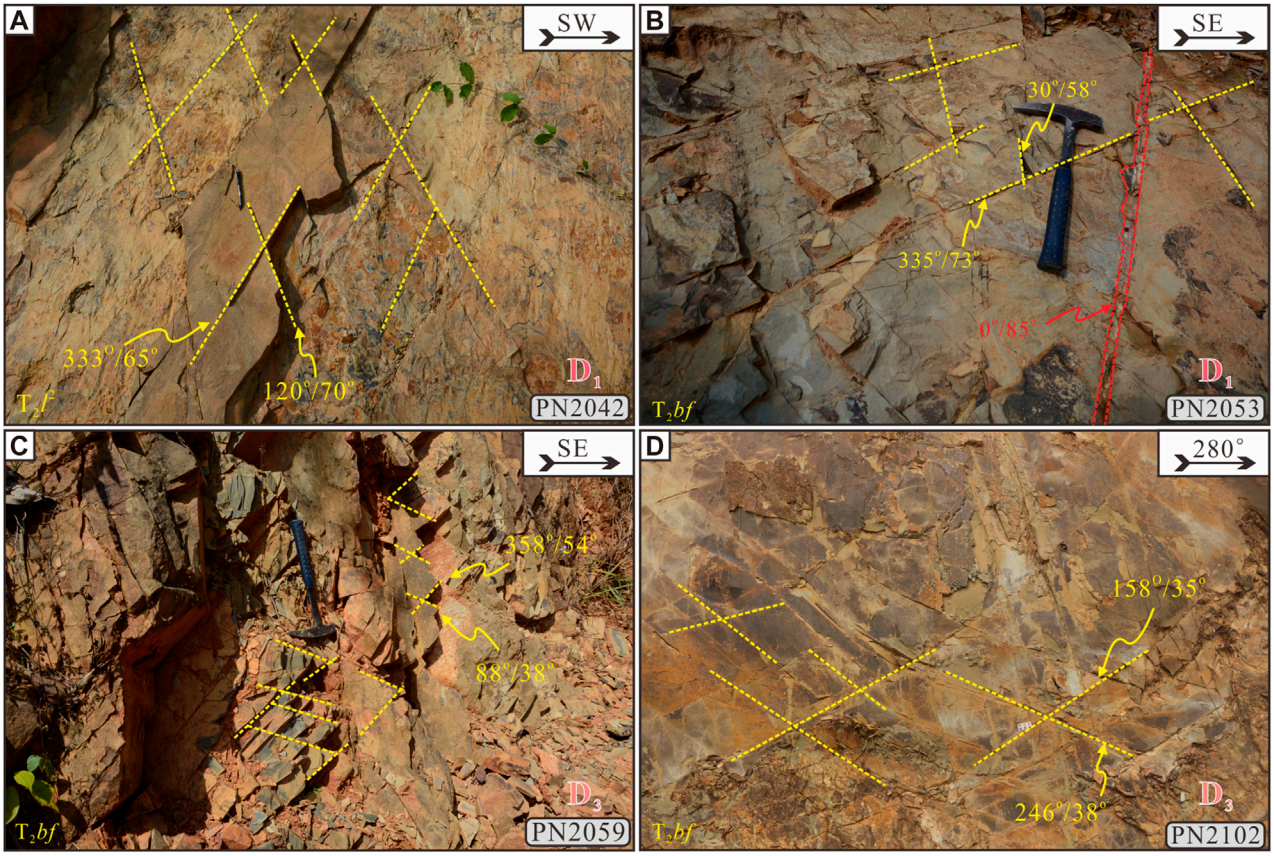

FIGURE 3
Field photographs of conjugate joints developed in the D_1 and D_3 structures in the YFTB. **(A)** Conjugated joints developed in the siltstones of the Triassic Lanmu Formation at PN2042 documenting NE–SW-oriented compression. **(B)** Conjugated joints developed in the siltstones of the Triassic Baifeng Formation at PN2053 indicating NE–SW-oriented compression. **(C)** Conjugated joints developed in the siltstones of the Triassic Baifeng Formation at PN2059 demonstrating NW–SE shortening. **(D)** Conjugated joints developed in the siltstone of the Triassic Lanmu Formation at PN2102 indicating NW–SE compression.

(σ1) (Arlegui and Simón, 2001; Wu et al., 2019). The dipping bedding with conjugate joints was calibrated to horizontal, and the corrected attitudes were then plotted in the rose diagram through Stereonet™ to determine their predominant direction and to infer the maximum principal stress (Allmendinger, 2002). The data of conjugate joints were presented in Supplementary Table S2.

Fault-related folds were also analyzed to determine the sense of thrusting. The overprinting relationships, including the fault plane crosscutting, striation superposition, and limitation between different sets of conjugate joints, were beneficial in deducing the sequence of the paleo-stress field.

Geometry and kinematic analysis

The study area is dominated by NW-trending folds and faults, which are locally crosscut by the NE-trending faults. The kinematic analysis indicates that the study area underwent polyphase tectonic movements. Based on the geometry, kinematic, and dynamic characteristic analysis of deformation conducted in the middle of the YFTB and the superposition and reworking relationships between these structural features, we have identified four phases of deformation with their paleo-stress field during the Mesozoic in the middle of the YFTB.

NE–SW shortening deformation (D_1)

The first phase of deformation (D_1), which established the tectonic framework in the study area, mainly consists of a NE-verging fold-and-thrust system in the Triassic and its underlying strata, such as the Tianlin synclinorium developed in the Tianlin district and the Lucheng–Tangxing fault outcropped around Baise city, as well as some strike-slip

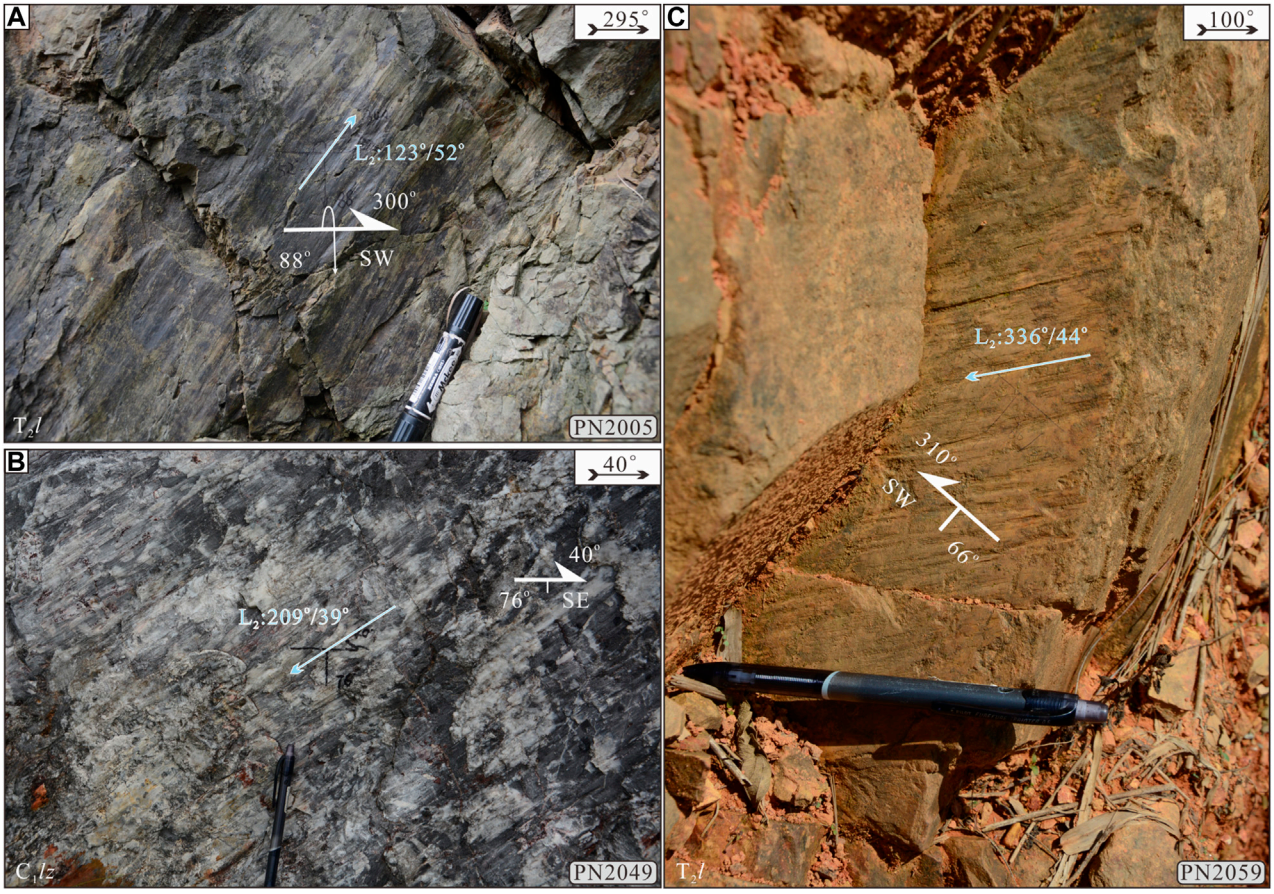

FIGURE 4
Field photographs of main structures developed in the D_2 deformation in the YFTB. **(A)** Sinistral striations and mineral steps on the hanging wall of the NW-striking fault plane in the siltstone of the Triassic Lanmu Formation at PN2005. The striations and mineral steps imply the top-to-the downward shear. **(B)** Striations and calcite mineral steps on the inter-bedding fault plane in the chert of the Carboniferous Luzhai Formation at PN2049 indicating a top-to-downward movement. **(C)** Striations developed on the NW-striking fault plane at PN2059 indicating top-to-downward movement.

faults. Most of these faults dip steeply and bear oblique-slip striations and mineral steps. Inversion results for the slip vectors show principal stress distributions of sub-horizontal σ1, sub-vertical σ2, and sub-horizontal σ3, indicating a NE–SW compression. This NE–SW-oriented compression regime has also been recorded by conjugate sets of NNE-striking dextral and E–W-striking strike-slip faults. The slip vector data from these fault planes demonstrate a NE–SW-oriented compressional regime that features sub-horizontal NE-trending σ1, sub-vertical σ2, and sub-horizontal NW-trending σ3 (Figures 2H–J). Similar kinematic characteristics are also manifested by the nearly dip-slip striations developed on the limb of the NW-trending fold (Figure 2K), with horizontal σ1, sub-horizontal σ2, and vertical σ3 indicating a NE–SW compression.

Furthermore, asymmetric fault-related folds with NW-striking hinges and NE- or SW-dipping axial planes are well developed in the study area, with gently dipping southern limbs and steeply dipping northern limbs, and *vice versa*, indicating a NE–SW trending compression. For example, the southern part of the NWW-trending Youjiang fault was outcropped and cut the Middle Triassic Baifeng Formation siltstone at PN2007 (Figure 2E), producing a series of fault-related folds. The asymmetric fault-related folds indicate a top-to-the-NE thrusting. The geometrical characteristics of other well-developed NW-trending folds also demonstrate a NE–SW-oriented shortening (Figures 2A–D,F,G).

In addition, plenty of conjugate joints developed in both limbs of the Tianlin synclinore in this regime (Figures 3A,B). The acute angle bisector between the joints indicates that they were formed by a NE–SW compression. Moreover, steeply-dipping cleavage (S_1) resulted from the D_1 deformation, which is well developed within the weak competent argillaceous layers in both limbs of the NW-trending folds. It transposes the

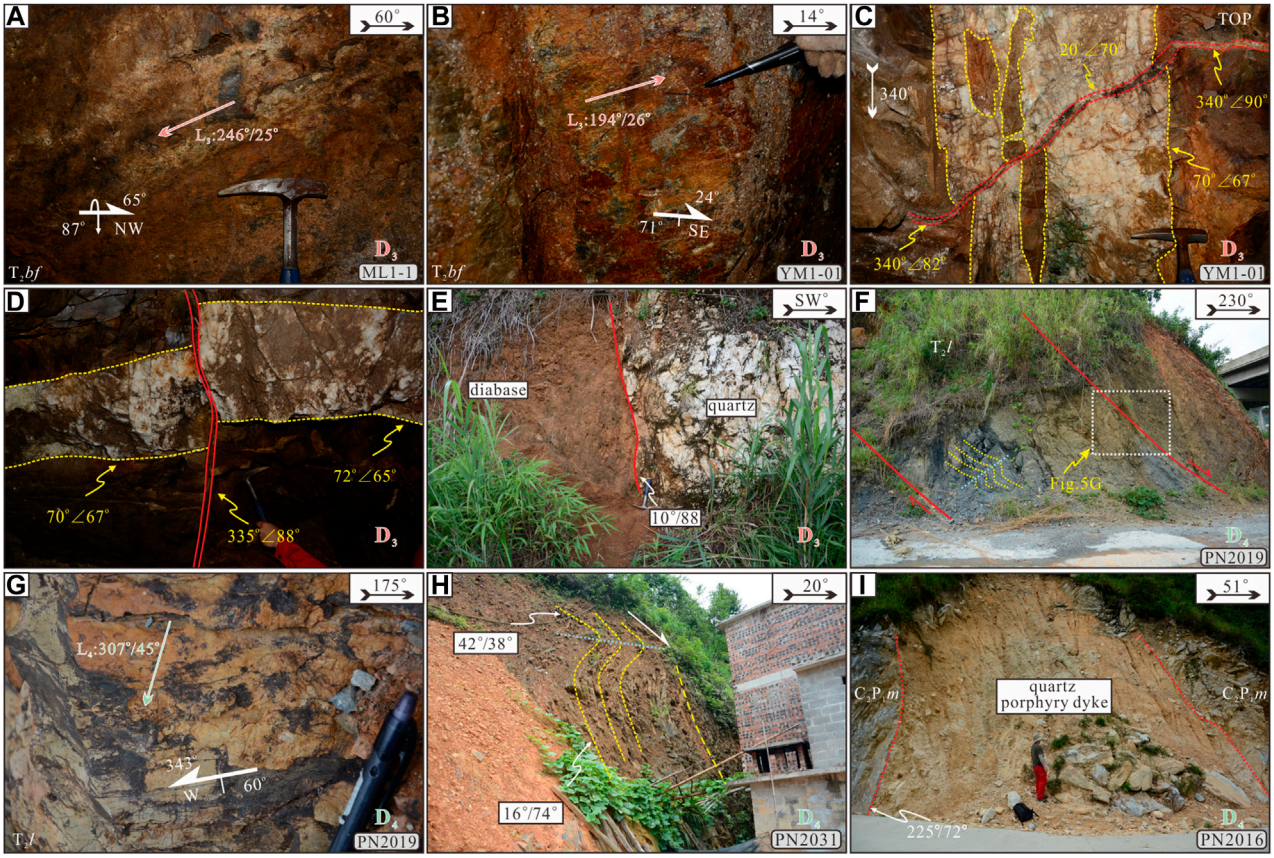

FIGURE 5
Field photographs of main structures and intrusions developed in the D_3 and D_4 structures in the YFTB. **(A)** Oblique striations on the NE-strike-slip fault plane in the siltstones of the Triassic Baifeng Formation at ML1-1 showing a NW–SE-oriented compression. **(B)** Strike-slip striations on the NNE-striking fault plane in the siltstones of the Triassic Baifeng Formation at YM1-01 indicating a NW–SE-oriented compression. **(C)** NW-striking fault crosscut NE-striking fault at YM1-01 in the Pingna underground tunnel. **(D)** NW-striking fault plane crosscut NE-striking fault in the Pingna underground tunnel. **(E)** NNE-striking fault crosscut the diabase that ourcropped in the Yangxu area. **(F)** The NW-striking normal fault and drag folds in the mudstones of the Triassic Lanmu Formation at PN2019 indicating nearly E–W-oriented extension. **(G)** The downward striations in the mudstones of the Triassic Lanmu Formation at PN2019 showing nearly E–W-oriented extension. **(H)** Asymmetric fold in Triassic siltstone at PN2031 implying the nearly E–W extension. **(I)** Quartz porphyry dyke intruded along the NW-striking fault. The fault crosscut the limestone of the Carboniferous Maping Formation at PN2016.

original bedding (S_0) and indicates an interlayer shearing (Figure 2L).

Nearly N–S extension (D_2)

This phase of deformation (D_2) is mostly manifested as the reworking of the pre-existing structures formed in the D_1 deformation, and it includes NW-trending normal faults and inter-bedding fractures developed on the limbs of NW-striking folds (Figure 4A).

Fault-related NE-verging folds developed along the NW-striking Liudan–Najin fault indicate that the NE–SW shortening coincides with the D_1 deformation (Figure 2C). The NW-trending fault is a sinistral fault dipping steeply with nearly dip-slip striations at PN2059, indicating that it was transposed by the D_2 deformation (Figure 4C). The fault slip vector is featured by horizontal σ1, sub-vertical σ2, and horizontal σ3, exhibiting a nearly N–S extension. The inter-bedding fault slip vectors developed on the Carboniferous chert at PN2049 record the same nearly N–S extension regime, with sub-vertical σ1, sub-horizontal σ2, and horizontal σ3 (Figure 4B).

In addition, diabase intrusions observed in the study area can provide constraints regarding the deformation timing (Figure 5E).

NW–SE shortening (D_3)

The third phase of deformation (D_3) is represented by the NE–SW-trending faults that crosscut previous NW–SE-

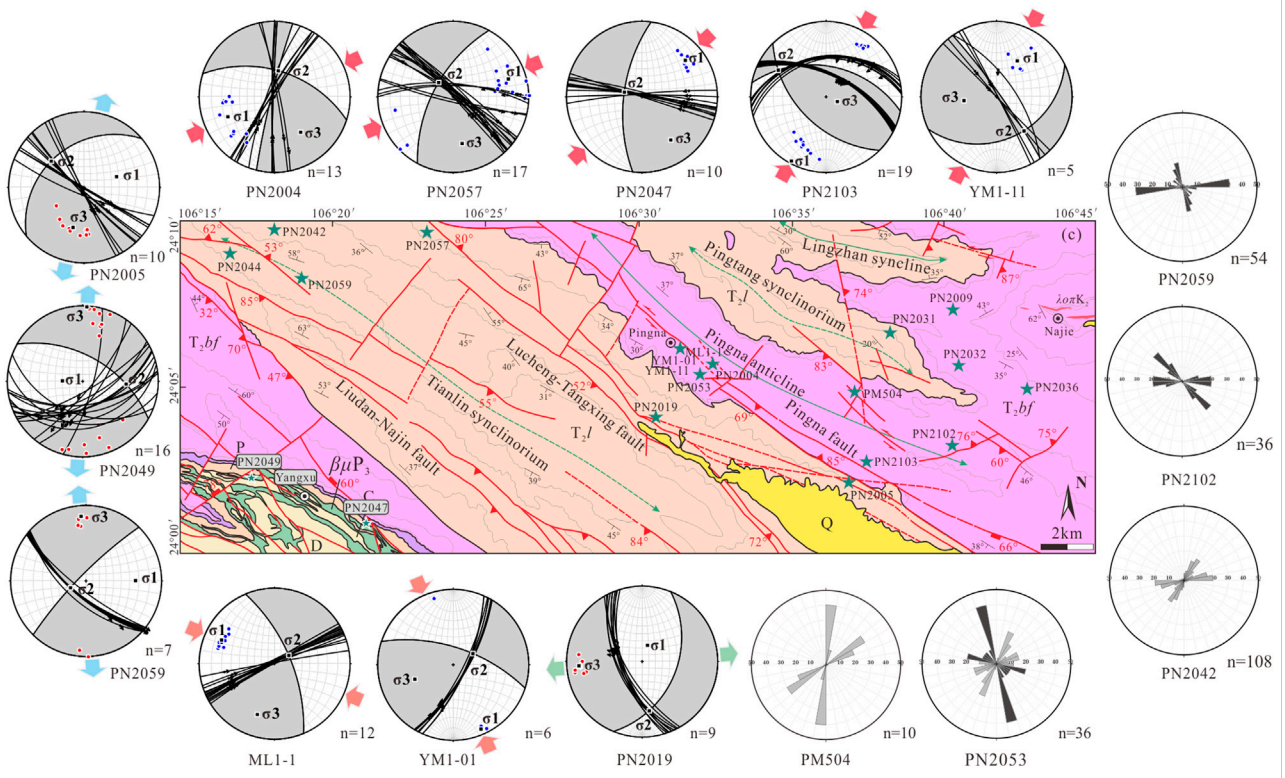

FIGURE 6
Stereographic plots of the main faults and conjugated joints in the study area. The observation points are shown with green pentagrams. The lower-hemisphere stereographic projection of brittle faults documents four phases of deformation and the rose diagram of conjugate documents a NE–SW and NW–SE compression regime.

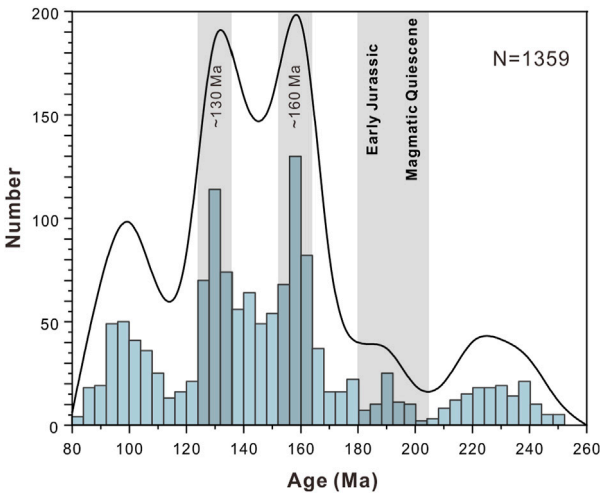

FIGURE 7
Age histogram of Mesozoic igneous rocks in the SCB. Age data are from Li and Li (2007), Gao et al. (2017), Gan et al. (2021), Li et al. (2021), and references therein. An apparent magmatic lull is inferred between the Late Triassic and the Early Jurassic.

striking thrust faults, the diabase, and a series of conjugate joints. A series of NE–SW-striking faults are observed in the underground tunnel of the Pingna deposit and crosscut the NW–SE-trending Pingna fault, indicating that they formed after the D_1 deformation (Figures 5A–D). The faults dip steeply with minor oblique-slip striations. Inversion results for the striations show a NW–SE compression that is characterized by a horizontal σ1, sub-horizontal σ2, and horizontal σ3 (Figures 5A,B, 6). This phase of deformation also crosscut the diabase formed at 249–187 Ma, indicating that it formed after the Early Jurassic (Figure 5E; Qiu et al., 2019).

Another set of conjugate joints was developed on the limbs of the Tianlin synclinorium (Figures 3C,D). The acute angle bisector between the joints indicates they were the product of the NW–SE compression (Figure 6). Regionally, the NE–SW-trending faults crosscut pre-existing NW–SE-striking faults formed in D_1 and the mafic rocks intruded in D_2 deformation.

As mentioned above, the structures formed in D_3 crosscut NW-striking faults formed in D_1 and overprint the structures and diabase formed in D_2, indicating that the NW–SE

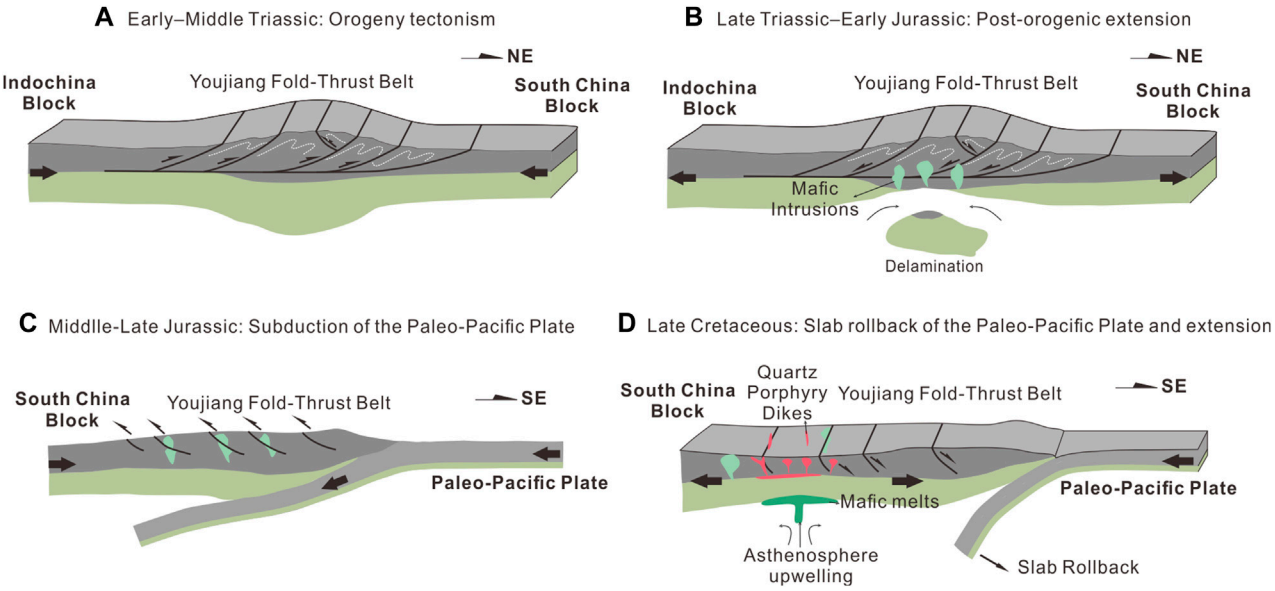

FIGURE 8
Tectonic model for the Mesozoic evolution of YFTB. **(A)** Collision between the Indochina block and SCB results in a series of NE-verging fold-and-thrust faults. **(B)** The delamination and post-collision rework the pre-existing structures and lead to the intrusion of mafic rocks. **(C)** The subduction of the Paleo-Pacific oceanic plate produces the N(N)E-striking faults that crosscut pre-existing structures and mafic rocks. **(D)** The rollback of the Paleo-Pacific plate leads to the back-arc extension setting and felsic dykes' emplacement. Modified from Qiu et al. (2019), Yang et al. (2021), and Zhang X. M. et al. (2021).

compression (D_3) occurred after NE–SW compression (D_1) and the nearly N–S extension and related structures (D_2).

Nearly E–W extension (D_4)

The fourth deformation (D_4) determined in the YFTB is characterized by several normal faults and lead to the Late Cretaceous W–Sn mineralization and quartz porphyry dyke emplacement. The normal faults are steeply dipping and have arrays of steeply dipping striations, with the inversion results documenting an extensional regime that features an E–W orientated σ3 (Figure 6).

The Youjiang fault outcrops in the Lanmu Formation, producing drag folds with gently dipping northeastern limbs, steeply dipping southwestern limbs, and NEE-dipping axial planes at PN2019. The geometrical characteristics of the drag fold indicate a nearly NEE–SWW extension (Figure 5F). The fault plane is steeply dipping with oblique-slip striations (l_4), documenting an extensional regime that features sub-vertical σ1, horizontal σ2, and horizontal σ3 (Figure 5G). Similar asymmetric fold are observed at PN2031 (Figure 5H). The striations (l_4) on the fault plane, together with the geometry characteristics of drag folds, suggest a nearly E–W-orientated extension.

Minor quartz porphyry dykes are exposed in the northeastern part of the study area. They intruded in the limestone of the Carboniferous Maping Formation (C_2P_1m) at PN2016 and in the siltstone of the Triassic Baifeng Formation (T_2bf) with NW-trending in the Najie area (Figure 5I). Previous studies have suggested that they were related to an extensional setting and formed in the Late Cretaceous (Chen et al., 2012; Zhu et al., 2017).

Discussion

Structural evolution of the Youjiang fold-and-thrust belt

The contraction of the Paleo-Tethys Ocean began through subduction in the Early Permian and mostly ended up with a closure in the Triassic (Wang et al., 2020; Feng et al., 2022). It induced the continental collision of the SCB with the Indochina block at Song Ma suture on the southern margin, causing extensive and intense intra-continental deformation in the SCB (Lin et al., 2008; Li S. Z. et al., 2017; Shu et al., 2021). The Indosinian orogeny generated the Late Triassic unconformity and pervasive E–W- and NW–SE-striking structures in the SCB, such as the intra-plate deformation of E–W-trending folds and faults widespread in the SCB (Zhang

et al., 2009), the NW–NWW-oriented thrust-and-fold sheets, and top-to-the-NE shearing reported in the Yunkai massif (Lin, 2008), NW–NWW- and E–W-trending faults and folds recorded in the Youjiang Basin and its adjacent region (Qiu, 2016; Yang et al., 2021), and the NW–SE-trending fold-and-thrust belt and ductile shearing zone outcropping in NE Vietnam (Lepvrier et al., 1997, 2011). The Indosinian orogeny also produced extensive magmatism in the SCB, which is distinguished from the Late Mesozoic magmatism by the quiescence between 205–180 Ma (Figure 7; Zhou et al., 2006). This tectonic event in the YFTB is characterized with prevailing NE- and NW-verging folds and NW-striking thrust faults (Figure 8A). The D_1 deformation, caused by the NE–SW-orientated compression and characterized by NE-verging fold-and-thrust, is consistent with the Indosinian orogeny (Figure 6).

Furthermore, previous research has suggested that the Indosinian magmatism in the SCB can be further divided into two stages (Mao et al., 2014). The early stage is considered as products of the collision between the Indochina block and the SCB with zircon U–Pb isotopic ages from 243 to 233 Ma, whereas the late stage occurred in a post-collisional extension setting with zircon U–Pb ages of 220–206 Ma (Sun et al., 2005; Wang et al., 2007b). In addition, Qiu et al. (2019) reported Early Jurassic mafic rocks linked to the post-orogenic extension in the Badu diabase with an LA–ICP–MS zircon U–Pb isotopic age of 187 Ma in the northwestern part of the study area. This extension may correspond to the D_2 deformation with nearly N–S-orientated extension in the YFTB (Figure 6), leading to the superimposition on pre-existing structures and mafic rocks emplacement (Figure 8B).

After the Indosinian orogeny, the SCB experienced the NW–SE compression due to the subduction of the Paleo-Pacific plate under the SCB (Figure 8C; Mao et al., 2014, 2021; Shu, 2021; Zhang et al., 2021; Shi et al., 2022). It produced a series of NE- to NNE-trending folds and thrust structures and vast intracontinental magmatism and structural belts in the SCB (Wang, 2013; Suo et al., 2019), which superimposed and reworked the Indosinian structures (Zhang, 2009). The same overprinting relationships have also been identified in the Youjiang Basin (Yang et al., 2021). In the YFTB, the D_3 deformation is represented by crosscutting between earlier NW–SE-striking faults and later NE–SW-striking faults. The D_3 NNE–SSW-trending faults also truncated the diabase that formed in D_2. These structural features are consistent with our investigations in the YFTB, indicating a NW–SE compression setting during the Middle Jurassic that resulted from the subduction of the Paleo-Pacific plate (Figure 6).

Along with the continuous subduction of the Paleo-Pacific plate and the subsequent high-angle subduction retreat or rollback, the SCB was dominated by an extensional setting (Figure 8D; Qiu et al., 2022a). It resulted in numerous extensional basins and domes and triggered intense magmatism and mineralization (Li et al., 2014). Coetaneous W–Sn mineralization and magmatism were mainly discovered along the boundary of the Youjiang Basin (Xiao et al., 2022). Minor igneous rocks outcropped in the interior of the basin including quartz porphyry dykes and (ultra-) mafic rocks (Chen, 2012). Chen et al. (2012) reported Ar^{40}–Ar^{39} ages of 96–95 Ma for muscovite from the quartz porphyry dykes. Zhu et al. (2017) determined zircon U–Pb ages for the quartz porphyry dykes of 99–95 Ma. These geochronological results indicated a Late Cretaceous magmatism in the Youjiang Basin and have been interpreted as the products of a lithospheric thinning and crustal extension event. Xiao et al. (2018) also reported LA–ICP–MS zircon U–Pb isotopic ages ranging from 93 to 92 Ma for the quartz porphyry, monzogranite, and biotite granite in the southeastern margin of the Youjiang Basin, inferring that they were linked to the extensional setting caused by the rollback of the Paleo-Pacific plate and the Neo-Tethys ocean slab. In the YFTB, sporadic quartz porphyry dykes intruded along the D_3 NW-trending faults (Figure 5I). The W–Sn ore-related granitoid and quartz porphyry dyke emplacement in the YFTB, together with these geochronological data, suggest that the YFTB experienced a nearly E–W-orientated extension (D_4) in the Late Cretaceous (Figure 6).

Two sets of conjugate joints recorded NW–SE and NE–SW compression. Integrated with regional geology, slickensides, fault-related folds, magmatic rocks, and their overprinting relationships, four phases of deformation in the Mesozoic have been recognized in the YFTB. D_1 and D_2 deformation were related to the Paleo-Tethys tectonic domain, and D_3 and D_4 deformation were associated with the Paleo-Pacific tectonic domain. The paleo-stress field and deformation characteristics in the YFTB demonstrate the Youjiang Basin was in a Paleo-Tethys-dominated setting as a foreland basin and then switched into the Paleo-Pacific domain, and the switch likely occurred between D_2 deformation, marked by the post-orogenic setting, and D_3, corresponding to the subduction of the Paleo-Pacific plate.

Tectonic implications

The Indosinian tectonic event was the most significant tectonic event in the Phanerozoic evolution history of the SCB and has essentially built up the structural architecture of the SCB (Wang et al., 2013; Li et al., 2017). Its occurrence could be constrained by the timing of the collision between the Sibumasu and Indochina blocks during 258–243 Ma (Carter et al., 2001; Lepvrier et al., 2004).

The Permian–Triassic tectono-magmatism in the SCB has been considered to be either associated with 1) the subduction of the Paleo-Tethys Ocean and the collision between the

Indochina and SCB (Jiang et al., 2015; Gao et al., 2017; Qiu et al., 2019) or 2) the subduction of the Paleo-Pacific plate (Li and Li, 2007; Shen et al., 2018). The hypothesis that the subduction of the Paleo-Pacific plate commenced in the Permian is supposed to produce a NW–SE compression, which contradicts the pervasive NW–SE-striking fold-and-thrust formed in D_1 deformation in the Youjiang Basin. In addition, this model cannot explain the absence of the Permian–Triassic subduction-related mafic rocks in the southeastern SCB (Gao et al., 2017). Niu et al. (2014) also noted that it would be theoretically difficult for a flat subduction to occur, especially on such a tremendous scale. Furthermore, Gan et al. (2021) identified apparent variations in geochemistry and rock associations and obvious magmatic quiescence between the Triassic and Early–Middle Jurassic magmatic rocks, implying that the transition commenced in the Early Jurassic. Zhou et al. (2006) recognized a relative quiescence in the SCB during the Early Jurassic (205–180 Ma), which is regarded as the transition timing of the SCB (Li S. Z. et al., 2017). In this study, we collected and summarized published geochronological data of the Mesozoic magmatism in the SCB and plotted them in a histogram. The statistical results indicated that there is an apparent quiescence between the Late Triassic and the Early Jurassic, followed by a magmatic peak at 160 Ma (205–180 Ma, Figure 7). A similar lull also existed in the mineralization in the SCB, which symbolizes the transition that occurred in the Early Jurassic (Zhao et al., 2022).

Li et al. (2017) identified the earlier NW-verging folds were overprinted by the NE-verging folds at the junction of the Youjiang Basin and Shiwandashan Basin, inferring that the subduction of the Paleo-Pacific plate was initiated in the Permian and facilitated the closure of the Paleo-Tethys Ocean. However, this kind of superposition is inconsistent with the deformation developed in the YFTB. On the contrary, Zhang et al. (2009) determined the superimposed relationship between the older nearly E–W-trending fold belt and younger NNE-trending fold in the SCB, proposing a transition from Paleo-Tethys to Paleo-Pacific tectonic domains in the Middle–Late Jurassic, combined with the strata contact and magmatism data.

Furthermore, Shu and Zhou (2002) considered that the Early–Middle Jurassic A-type granites and bimodal volcanic rocks in the Jurassic basin in the Nanling region marked the transition in the southeastern SCB. Li S. Z. et al. (2017) believed that different transitions happened in the SCB, including the Late Triassic in the Xuefengshan region and Early–Middle Jurassic in the Nanling region. In summary, the Early Jurassic was a significant changing period both for magmatism and structural features in the SCB.

The deformation features and overprinting relationships in the YFTB are pervasive in the SCB and the evolution of four phases of deformation in the YFTB witnessed the transition of two tectonic domains. The paleo-stress field and deformation characteristics in the YFTB demonstrate that the Youjiang Basin was in a Paleo-Tethys-dominated setting as a foreland basin in the Triassic. The quiescence of the magmatism and mineralization is compelling evidence to constrain the transition timing, which suggests the SCB likely experienced a transition from the Paleo-Tethys to the Paleo-Pacific tectonic domains in the Early Jurassic (Figure 8C).

Conclusion

1) Our structural analysis and paleo-stress field inversion, together with regional geology, determined the deformation sequence in the YFTB during the Mesozoic. Four phases of deformation are identified, including NE–SW shortening deformation (D_1) in the Permian–Middle Triassic, nearly N–S extension (D_2) in the Late Triassic, NW–SE shortening (D_3) in the Jurassic, and nearly E–W extension (D_4) in the Cretaceous.
2) D_1 and D_2 deformation corresponded to the collision and post-collision stages in the Indosinian orogeny, respectively. D_3 and D_4 deformation were respectively associated with the subduction of the Paleo-Pacific plate and slab-rollback in the Yanshanian tectonic event (Jurassic to Cretaceous).
3) Our study suggests that the tectonic transition of the SCB in response to the subduction of the Paleo-Pacific plate more likely occurred in the Early Jurassic, not the Permian.

Data availability statement

The original contributions presented in the study are included in the article/Supplementary Material; further inquiries can be directed to the corresponding author.

Author contributions

J-XH collected the data for analysis, and compiled the results and wrote the manuscript. J-XH also finished the figures and table. C-HX designed the study, collected the data for analysis, and compiled the results and wrote the manuscript. C-SW, Y-KS, Z-LC, and YZ collected the data for analysis and provided feedback to the manuscript. DZ provided feedback to the manuscript.

Funding

This study was financially supported by the Basic Research Fund of the Chinese Academy of Geological Sciences (Grant: DZLXJK202203) and the China Geological Survey (Grants: DD20190161; DD20221660-3).

Acknowledgments

Richard W. Allmendinger is thanked for sharing the structural software *FaultKin* and *Stereonet*. We sincerely thank the Guest Editor FY, the reviewer LQ, and the other two reviewers for their hard work and constructive comments that have improved the quality of our paper.

Conflict of interest

The authors declare that the research was conducted in the absence of any commercial or financial relationships that could be construed as a potential conflict of interest.

Publisher's note

All claims expressed in this article are solely those of the authors and do not necessarily represent those of their affiliated organizations, or those of the publisher, the editors and the reviewers. Any product that may be evaluated in this article, or claim that may be made by its manufacturer, is not guaranteed or endorsed by the publisher.

Supplementary material

The Supplementary Material for this article can be found online at: https://www.frontiersin.org/articles/10.3389/feart.2022.1033541/full#supplementary-material

References

Allmendinger, R. W. (2002). *Stereonet V. 1.1.6 and FaultKin V. 1.2.2.* Ithaca, New York shareware software: Cornell University, Department of Geological Sciences. geo. cornell.edu/pub/rwa.

Angelier, J. (1984). Tectonic analysis of fault slip data sets. *J. Geophys. Res.* 89, 5835–5848. doi:10.1029/JB089iB07p05835

Arlegui, L., and Simón, J. L. (2001). Geometry and distribution of regional joint sets in a non-homogeneous stress field: Case study in the Ebro basin (Spain). *J. Struct. Geol.* 23, 297–313. doi:10.1016/S0191–8141(00)00097–3

Carter, A., Roques, D., Bristow, C., and Kinny, P. (2001), .Understanding Mesozoic accretion in southeast Asia: Significance of Triassic thermotectonism (Indosinian orogeny) in Vietnam, *Geology*, 29, 2112–2214. doi:10.1130/0091-7613(2001)029<0211

Chen, C. H., Lee, C. Y., and Shinjo, R. (2008). Was there Jurassic paleo-pacific subduction in South China? Constraints from $^{40}Ar/^{39}Ar$ dating, elemental and Sr-Nd-Pb isotopic geochemistry of the Mesozoic basalts. *Lithos* 106, 83–92. doi:10.1016/j.lithos.2008.06.009

Chen, H. D., and Zeng, Y. F. (1990). [Evaluation of effects of dust prevention in the principal tungsten mines in Jiangxi]. *Zhonghua Yu Fang. Yi Xue Za Zhi* 10, 28–30. (in Chinese). doi:10.16108/j.issn1006-7493.2012.01.011

Chen, M. H., Lu, G., and Li, X. H. (2012). Muscovite 40Ar/39Ar dating of the quartz porphyry veins from Northwest Guangxi, China, and its geological significance. *Geol. J. China Univ* 1, 106–116. (in Chinese with English abstract).

Du, Y. S., Huang, H., Yang, J. H., Huang, H. W., Tao, P., Huang, Z. Q., et al. (2013). The basin translation from the late Paleozoic to Triassic of the Youjiang basin and its tectonic signification. *Geol. Rev.* 59, 1–11. (in Chinese). doi:10.16509/j.georeview.2013.01.009

Duan, L., Meng, Q. R., Wu, G. L., Yang, Z., Wang, J. Q., and Zhan, R. R. (2020). Nanpanjiang basin: A window on the tectonic development of South China during Triassic assembly of the southeastern and eastern Asia. *Gondwana Res.* 78, 189–209. doi:10.1016/j.gr.2019.08.009

Faure, M., Lepvrier, C., Nguyen, V., Vu, T., Lin, W., and Chen, Z. (2014). The South China block-Indochina collision: Where, when, and how? *J. Asian Earth Sci.* 79, 260–274. doi:10.1016/j.jseaes.2013.09.022

Feng, H. W., Xu, S. M., Wang, J. D., Zhang, G. L., Zeng, Z. P., and Shu, P. C. (2022). Jurassic provenances and their transition mechanism of the Delingha Sag in the eastern segment of northern margin of the Qaidam Basin, North Tibet. *Geosystems Geoenvironment* 1, 100097. doi:10.1016/j.geogeo.2022.100097

Gan, C. S., Zhang, Y. Z., Wang, Y. J., Qian, X., and Wang, Y. (2021). Reappraisal of the Mesozoic tectonic transition from the Paleo-Tethyan to Paleo-Pacific domains in South China. *Bull. Geol. Soc. Am.* 133, 2582–2590. doi:10.1130/B35755.1

Gao, P., Zheng, Y. F., and Zhao, Z. F. (2017). Triassic granites in South China: A geochemical perspective on their characteristics, petrogenesis, and tectonic significance. *Earth. Sci. Rev.* 173, 266–294. doi:10.1016/j.earscirev.2017.07.016

Hu, L. S., Cawood, P. A., Du, Y. S., Yang, J. H., and Jiao, L. X. (2015). Late Paleozoic to early Mesozoic provenance record of paleo-Pacific subduction beneath South China. *Tectonics* 34, 986–1008. doi:10.1002/2014TC003803

Jiang, W., Yan, Q. R., Deng, L., Zhou, B., Xiang, Z. J., and Xia, W. J. (2019). Early Jurassic mafic intrusions in the southern Youjiang Basin, SW China: Petrogenesis, tectonic and metallogenic implications. *Minerals* 9, 771. doi:10.3390/min9120771

Jiang, Y. H., Wang, G. C., Liu, Z., Ni, C. Y., Qing, L., and Zhang, Q. (2015). Repeated slab advance-retreat of the Palaeo-Pacific plate underneath SE China. *Int. Geol. Rev.* 57, 472–491. doi:10.1080/00206814.2015.1017775

Lehrmann, D., Chaikin, D., Enos, P., Minzoni, M., Payne, J., Yu, Y., et al. (2015). Patterns of basin fill in Triassic turbidites of the Nanpanjiang basin: Implications for regional tectonics and impacts on carbonate-platform evolution. *Basin Res.* 27 (5), 587–612. doi:10.1111/bre.12090

Lepvrier, C., Maluski, H., Van Tich, Vu, Leyreloup, A., Truong Thi, P., and Van Vuong, N. (2004). The early Triassic Indosinian orogeny in Vietnam (Truong Son belt and Kontum Massif): Implications for the geodynamic evolution of Indochina. *Tectonophysics* 393, 87–118. doi:10.1016/j.tecto.2004.07.030

Lepvrier, C., Faure, M., Van, V. N., Vu, T., Van Lin, W., Trong, T. T., et al. (2011). North-directed Triassic nappes in northeastern Vietnam (East Bac Bo). *J. Asian Earth Sci.* 41, 56–68. doi:10.1016/j.jseaes.2011.01.002

Lepvrier, C., Maluski, H., Vuong, N. Van, Roques, D., Axente, V., and Rangin, C. (1997). Indosinian NW-trending shear zones within the Truong Son belt (Vietnam) ^{49}Ar-^{39}Ar Triassic ages and Cretaceous to Cenozoic overprints. *Tectonophysics* 283, 105–127. doi:10.1016/S0040-1951(97)00151-0

Li, C. L., Wang, Z. X., Lü, Q. T., Tan, Y. L., Li, L. L., and Tao, T. (2021). Mesozoic tectonic evolution of the eastern South China block: A review on the synthesis of the regional deformation and magmatism. *Ore Geol. Rev.* 131, 104028. doi:10.1016/j.oregeorev.2021.104028

Li, J. H., Zhang, Y. Q., Dong, S. W., and Johnston, S. T. (2014a). Cretaceous tectonic evolution of South China: A preliminary synthesis. *Earth. Sci. Rev.* 134, 98–136. doi:10.1016/j.earscirev.2014.03.008

Li, J. H., Zhao, G. C., Johnston, S. T., Dong, S. W., Zhang, Y. Q., Xin, Y. J., et al. (2017). Permo-Triassic structural evolution of the Shiwandashan and Youjiang structural belts, South China. *J. Struct. Geol.* 100, 24–44. doi:10.1016/j.jsg.2017.05.004

Li, S. Z., Zang, Y. B., Wang, P. C., Suo, Y. H., Li, X. Y., Liu, X., et al. (2017a). Mesozoic tectonic transition in South China and initiation of Palaeo-Pacific subduction. *Earth Sci. Front.* 24 (4), 213–225. (in Chinese with English abstract). doi:10.13745/j.esf.yx.2017–4–13

Li, Z. X., Li, X. H., Chung, S. L., Lo, C. H., Xu, X. S., and Li, W. X. (2012). Magmatic switch-on and switch-off along the South China continental margin since the Permian: Transition from an Andean-type to a Western Pacific-type plate boundary. *Tectonophysics* 532–535, 271–290. doi:10.1016/j.tecto.2012.02.011

Li, Z. X., and Li, X. H. (2007). formation of the 1300-km-wide intracontinental orogen and postorogenic magmatic province in Mesozoic South China: A flat-slab subduction model. *Geol.* 35, 179–182. doi:10.1130/G23193A.1

Lin, W., Wang, Q. C., and Chen, K. (2008). Phanerozoic tectonics of South China block: New insights from the polyphase deformation in the Yunkai massif. *Tectonics* 27, 1–16. doi:10.1029/2007TC002207

Mao, J. R., Li, Z. L., and Ye, H. M. (2014). Mesozoic tectono-magmatic activities in South China: Retrospect and prospect. *Sci. China Earth Sci.* 57, 2853–2877. doi:10.1007/s11430-014-5006-1

Meng, L. F., Li, Z. X., Chen, H. L., Li, X. H., and Wang, X. C. (2012). Geochronological and geochemical results from Mesozoic basalts in southern South China block support the flat-slab subduction model. *Lithos* 132 (133), 127–140. doi:10.1016/J.LITHOS.2011.11.022

Niu, Y. L. (2014). Geological understanding of plate tectonics: Basic concepts, illustrations, examples and new perspectives. *gtm.* 10, 23–46. doi:10.1127/gtm/2014/0009

Qiu, L., Kong, R. Y., Yan, D. P., Mu, H. X., Sun, W. H., Sun, S. H., et al. (2022a). Paleo–Pacific plate subduction on the eastern Asian margin: Insights from the Jurassic foreland system of the overriding plate. *GSA Bull.* 134, 2305–2320. doi:10.1130/b36118.1

Qiu, L., Yan, D. P., Tang, S. L., Chen, F., Song, Z. D., Gao, T., et al. (2020). Insights into post-orogenic extension and opening of the Palaeo-Tethys Ocean recorded by an Early Devonian core complex in South China. *J. Geodyn.* 135, 101708. doi:10.1016/j.jog.2020.101708

Qiu, L., Yan, D. P., Tang, S. L., Wang, Q., Yang, W. X., Tang, X. L., et al. (2016). Mesozoic geology of southwestern China: Indosinian foreland overthrusting and subsequent deformation. *J. Asian Earth Sci.* 122, 91–105. doi:10.1016/j.jseaes.2016.03.006

Qiu, L., Yang, W. X., Yan, D. P., Wells, M. L., Qiu, J. T., Gao, T., et al. (2019). Geochronology of early Mesozoic diabase units in southwestern China: Metallogenic and tectonic implications. *Geol. Mag.* 156, 1141–1156. doi:10.1017/S0016756818000493

Shen, L. W., Yu, J. H., O'Reilly, S. Y., Griffin, W. L., and Zhou, X. Y. (2018). Subduction-related middle Permian to early Triassic magmatism in Central Hainan Island, South China. *Lithos* 318–319, 158–175. doi:10.1016/j.lithos.2018.08.009

Shi, W., Dong, S. W., and Zhang, Y. Q. (2022). Jurassic contractional deformation in the central–Western North China craton in response to multi-plate convergence in the East Asia. *Geosys. Geoenviron.*, 100099. doi:10.1016/j.geogeo.2022.100099

Shu, L. S., Yao, J. L., Wang, B., Faure, M., Charvet, J., and Chen, Y. (2021). Neoproterozoic plate tectonic process and Phanerozoic geodynamic evolution of the South China block. *Earth. Sci. Rev.* 216, 103596. doi:10.1016/j.earscirev.2021.103596

Shu, L. S., and Zhou, X. M. (2002). Late Mesozoic tectonism of southeast China. *Geol. Rev.* 48 (3), 249–260. (in Chinese with English abstract).

Sun, T., Zhou, X. M., Chen, P. R., Li, H. M., Zhou, H. Y., Wang, Z. C., et al. (2005). Strongly peraluminous granites of Mesozoic in eastern Nanling range, southern China: Petrogenesis and implications for tectonics. *Sci. China Ser. D-Earth. Sci.* 48, 165–174. doi:10.1360/03YD0042

Suo, Y. H., Li, S. Z., Jin, C., Zhang, Y., Zhou, J., Li, X. Y., et al. (2019). Eastward tectonic migration and transition of the Jurassic-Cretaceous Andean-type continental margin along Southeast China. *Earth. Sci. Rev.* 196, 102884. doi:10.1016/j.earscirev.2019.102884

Wang, Q. F., Yang, L., Xu, X. J., Santosh, M., Wang, Y. N., Wang, T. Y., et al. (2020). Multi–stage tectonics and metallogeny associated with phanerozoic evolution of the South China block: A holistic perspective from the Youjiang Basin. *Earth. Sci. Rev.* 211, 103405. doi:10.1016/j.earscirev.2020.103405

Wang, Y. J., Fan, W. M., Sun, M., Liang, X. Q., Zhang, Y. H., and Peng, T. P. (2007). Geochronological, geochemical and geothermal constraints on petrogenesis of the Indosinian peraluminous granites in the South China block: A case study in the Hunan Province. *Lithos* 96, 475–502. doi:10.1016/j.lithos.2006.11.010

Wang, Y. J., Fan, W. M., Zhang, G. W., and Zhang, Y. H. (2013). Phanerozoic tectonics of the South China block: Key observations and controversies. *Gondwana Res.* 23, 1273–1305. doi:10.1016/j.gr.2012.02.019

Wang, Y. N., Wang, Q. F., Deng, J., Xue, S. C., Li, C. S., and Ripley, E. M. (2021). Late Permian-Early Triassic mafic dikes in the southwestern margin of the South China block: Evidence for Paleo-Pacific subduction. *Lithos* 105994, 384–385. doi:10.1016/j.lithos.2021.105994

Wang, Y. J., Zhang, F. F., Fan, W. M., Zhang, G. W., Chen, S. Y., Cawood, P. A., et al. (2010). Tectonic setting of the South China Block in the early Paleozoic: Resolving intracontinental and ocean closure models from detrital zircon U-Pb geochronology. *Tectonics* 29. doi:10.1029/2010TC002750

Wu, Y., Zhang, S., Huang, Z., Wang, F., Li, J., Xiao, C., et al. (2019). Meso-Cenozoic tectonic evolution of the Nandan-Libo area, northwestern Guangxi, China: Evidence from palaeo-tectonic stress fields analyses. *Geotecton. Metallog.* 43, 872–893. doi:10.16539/j.ddgzyckx.2019.05.002

Xiao, C. H., Chen, Z. L., Liu, X. C., Wei, C. S., Wu, Y., Tang, Y. W., et al. (2022). Structural analysis, mineralogy, and cassiterite U–Pb ages of the Wuxu Sb-Zn-polymetallic district, Danchi Fold-and-Thrust belt, South China. *Ore Geol. Rev.* 150, 105150. doi:10.1016/j.oregeorev.2022.105150

Xiao, C. H., Shen, Y. K., Wei, C. S., Su, X. K., Le, X. W., and Zhang, L. (2018). LA–ICP–MS zircon U–Pb dating, Hf isotopic composition and Ce4+/Ce3+ characteristics of the Yanshanian acid magma in the Xidamingshan cluster, southeastern margin of the Youjiang fold belt, Guangxi. *Geoscience* 32 (2), 289–304. (in Chinese with English abstract).

Xu, C. H., Zhang, L., Shi, H. S., Brix, M. R., Huhma, H., Chen, L. H., et al. (2017). Tracing an early Jurassic magmatic arc from South to East China Seas. *Tectonics* 36, 466–492. doi:10.1002/2016TC004446

Xu, X. B., Li, Q. M., Gui, L., Su, Y. P., and Zhang, X. F. (2019). Early Mesozoic tectonic transition of the eastern South China block: Constraints from late Triassic Dashuang complex in Eastern Zhejiang Province. *Int. Geol. Rev.* 61, 997–1015. doi:10.1080/00206814.2018.1490931

Yang, L., Deng, J., Groves, D. I., Wang, Q. F., Zhang, L., Wu, W., et al. (2020). Recognition of two contrasting structural- and mineralogical-gold mineral systems in the Youjiang basin, China-Vietnam: Orogenic gold in the south and Carlin-type in the north. *Geosci. Front.* 11, 1477–1494. doi:10.1016/j.gsf.2020.05.011

Yang, W. X., Yan, D. P., Qiu, L., Wells, M. L., Dong, J. M., Gao, T., et al. (2021). formation and forward propagation of the Indosinian foreland fold-thrust belt and Nanpanjiang foreland basin in SW China. *Tectonics* 40, 1–24. doi:10.1029/2020TC006552

Zeng, Y. F., Liu, W. J., Chen, H. D., Zheng, R. C., Zhang, J. Q., Li, X. Q., et al. (1995). Evolution of sedimentation and tectonics of the Youjiang composite basin, South China. *Acta Geol. Sin.* 69 (2), 113–124. (in Chinese).

Zhang, D., Li, F., He, X. L., Hu, B. J., Zhang, X. M., Bi, M. F., et al. (2021). Mesozoic tectonic deformation and its rock/ore-control mechanism in the important metallogenic belts in South China. *J. Geomech.* 27 (4), 497–506. (in Chinese with English abstract). doi:10.12090/j.issn.1006-6616.2021.27.04.045

Zhang, G. W., Guo, A. L., Wang, Y. J., Li, S. Z., Dong, Y. P., Liu, S. F., et al. (2013). Tectonics of South China continent and its implications. *Sci. China Earth Sci.* 56, 1804–1828. doi:10.1007/s11430-013-4679-1

Zhang, X. M., Zhang, D., Bi, M. F., Wu, G. G., Fan, Z. Z., Que, C. Y., et al. (2021). Genesis and geodynamic setting of the Nanyangtian tungsten deposit, SW China: Constraints from structural deformation, geochronology, and S–O isotope data. *Ore Geol. Rev.* 138, 104354. doi:10.1016/j.oregeorev.2021.104354

Zhang, Y. Q., Dong, S. W., Li, J. H., Cui, J. J., Shi, W., Su, J. B., et al. (2012). The new progress in the study of Mesozoic tectonics of South China. *Acta Geol. Sin.* 33, 257–279. (in Chinese with English abstract).

Zhang, Y. Q., Xu, X. B., Jia, D., and Shu, L. S. (2009). Deformation record of the change from Indosinian collision-related tectonic system to Yanshanian subduction-related tectonic system in South China during the Early Mesozoic. *Earth Sci. Front.* 16 (1), 234–247. (in Chinese with English abstract).

Zhao, Z., Chen, Y. C., Wang, D. H., Li, J. K., Liu, S. B., Chen, Z. Y., et al. (2022). Transformation of Mesozoic dynamic systems and superposition of metallogenic series of W-Sn-Li-Be-Nb-Ta-REE mineral deposits in South China. *Acta Petrol. Sin.* 38 (2), 301–322. (in Chinese with English abstract). doi:10.18654./1000–0569./2022.02.01

Zhou, X. M., Sun, T., Shen, W. Z., Shu, L. S., and Niu, Y. L. (2006). Petrogenesis of Mesozoic granitoids and volcanic rocks in South China: A response to tectonic evolution. *Episodes* 29, 26–33. doi:10.18814/epiiugs/2006/v29i1/004

Zhu, J. J., Hu, R. Z., Richards, J. P., Bi, X. W., Stern, R., and Lu, G. (2017). No genetic link between Late Cretaceous felsic dikes and Carlin–type Au deposits in the Youjiang basin, Southwest China. *Ore Geol. Rev.* 84, 328–337. doi:10.1016/j.oregeorev.2017.01.014